ELSEVIER

Journal of Photochemistry and Photobiology A: Chemistry 113 (1998) 125–134

Journal of Photochemistry and Photobiology A:Chemistry

Emission quenching via intramolecular electron transfer for fluorescein conjugates. Dependences on driving force and medium

Guilford Jones II *, Xiaohua Qian

Department of Chemistry, and the Center for Photonics, Boston University, Boston, MA 02215, USA

Abstract

The fluorescence properties of conjugates of the dye, fluorescein, in which triazine or dinitrobenzoyl groups are attached to an amine function in the 5′ position have been studied. The substantial quenching of fluorescence which is observed with this modification is attributed to intramolecular electron transfer involving the xanthene moiety as electron donor (i.e., the shift of anionic charge). The fluorescein dianion which is important for neutral water solutions is more effective as an electron donor on comparison with the monoanion, as determined by the dependence of fluorescence quenching on pH. Binding of the conjugates to poly(vinyl-2-pyrrolidone) (PVP), a domain-forming polymer in water, leads to alterations of fluorescence spectra as well as changes in emission quantum yields and lifetimes. Fluorescence probes that are based on the mediation of emission properties by intramolecular electron transfer are discussed.

Keywords: Fluorescence; Electron donor; Conjugate

1. Introduction

A continuing interest in our laboratory involves the study of linked electron donor–acceptor systems capable of binding to proteins or to domain-forming polymers in water [1–3]. Systems of this type are important in part because they provide models for the behavior of natural redox systems such as photosynthetic reaction centers [4]. The general expectation is that photochemical and photophysical properties can be significantly altered on binding a donor–acceptor 'photoligand' (D–A) to a (bio)polymer microdomain (Scheme 1). In principle, the binding sites of macromolecules will play a role in controlling rates of intramolecular electron transfer through adjustments in microscopic polarity and other properties of the medium. Local effects associated with the binding of ligands within (bio)polymer microdomains may arise as the result of local charge distributions, and specific hydrophobic or hydrogen bonding interactions. Alterations of the microenvironment in turn may influence D–A electronic coupling, or the driving forces and medium reorganization energies associated with electron transfer [5]. Recent examples of studies in which a non-native photoligand has been introduced to a protein microenvironment include the incorporation in serum albumin of an aminonaphthalene-sulfonate linked to a nitroxide electron acceptor [6]. Other studies have focused on the effects of microenvironment on electron transfer events that take place between a non-covalent ligand and a redox active group that is native to a protein [7,8].

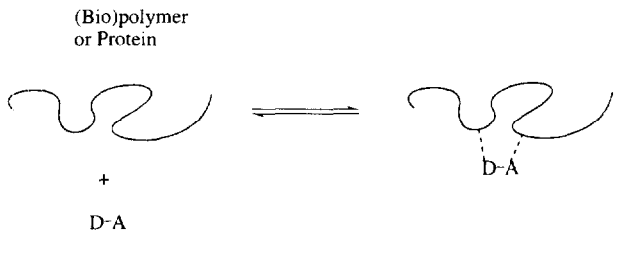

Scheme 1.

Fluorescein (**1**) and its simple derivatives have proved to be among the most versatile of chromophores used as fluorescence probes. The free dye, or dye in derivatized form, is used widely as a tracer in the labeling of proteins [9]. Recent applications employ **1** to probe the structure of cells or to measure pH at the interface of surfaces at which dye is immobilized [10,11]. In 1990, Munkholm et al. [12] reported on the mediation of the fluorescence of fluorescein that results from attachment of electron donor groups to the 5′ position of the benzoate ring of the substituted xanthene structure. In this study the titration behavior of fluoresceinamine (**2**) and the pattern of substituent influences were consistent with a

* Corresponding author.

1010-6030/98/$19.00
PII S1010-6030(97)00326-2

mechanism of emission quenching associated with electron transfer. It was further shown that the competition from a non-radiative decay path in which an electron is transferred from the aniline moiety to the photoexcited xanthene ring can be significantly reversed on binding **2** to surfactants in water (e.g., cetyltrimethylammonium bromide, CTAB). Substitution with nitro groups in the benzoate ring of fluorescein also led to fluorescence quenching, a finding ascribed to possible substituent influences that enhance intersystem crossing yielding dye triplets [12].

In the present study, another type of mediated fluorescence for fluorescein has been studied in detail. The quenching of emission has been observed for two derivatives in which 5′-[(4,6-dichlorotriazinyl)-amino] (**3**) and 5′-[(3,5-dinitrobenzoyl)amido] (**4**) groups are attached. Through the measurement of quantum yields and emission lifetimes, and their dependence on the structure of conjugates, medium pH and other factors, it has been possible to show that electron transfer is the important quenching mechanism. For these conjugates, electron transfer occurs in a sense that is reversed, relative to that for **2**; i.e., the xanthene ring serves as electron donor and the 5′ substituents serve as acceptors. We show further that the quenching behavior is dependent on medium in several ways. For example, the dianion form of fluorescein, a more effective electron donor, is subject to greater quenching relative to the monoanion, the dye species which is important for aqueous media at pH = ca. 5.0.

An effort has also been made to quantify special medium effects associated with the interaction of **3** and **4** with a water-soluble vinyl polymer. On binding the conjugates to the domain-forming polymer, poly(vinyl-2-pyrrolidone) (PVP) [13], in water, fluorescence is substantially restored. The case is made that the polymer domain provides a local environment that is less favorable for electron transfer (e.g., an influence on medium reorganization energy). The conjugates, **3** and **4**, are thus effective probes of polymer binding and polymer microenvironment through observation of the recovery of emission.

Other cases of mediated fluorescence for conventional chromophores that have been studied in our laboratory include the conjugates of another dye of the xanthene family, eosin, and amino acids and peptides containing tryptophan or tyrosine [1,2]. 9-Substituted acridinium ions [3,14,15], and tryptophan-containing peptides which have been modified with the pyrenesulfonyl moiety [16] also give rise to fluorescence that is highly sensitive to structure and medium influences, due to the importance of intramolecular electron transfer.

2. Experimental

2.1. Materials

5′-[(4,6-Dichlorotriazin-2-yl)amino]fluorescein hydrochloride (**3**) was purchased from Acros Organics; its purity was confirmed by thin layer chromatography. 5′-[(3,5-Dinitrobenzoyl)amido]-fluorescein (**4**) was synthesized using fluoresceinamine, isomer I (**2**, purchased from Aldrich and used as received) and 3,5-dinitrobenzoyl chloride, 98+% (Aldrich). The solvents, methanol, acetone, and ethyl ether were from J.T. Baker, (ACS grade); 100% ethanol was from Pharmoco. The dye, fluorescein, was purchased from Eastman Kodak and was recrystallized from acetone twice before use. The polymer, poly(vinyl-2-pyrrolidone) (PVP) (M.W. = 360,000) was obtained from Aldrich and used without further purification [1,2].

2.2. 5′-[(3,5-Dinitrobenzoyl)amido]fluorescein (4)

3,5-Dinitrobenzoyl chloride (200 mg, 0.87 mmol) dissolved in 1.5 ml of DMF was added to 2.0 ml of a DMF solution of fluoresceinamine, isomer I (300 mg, 0.86 mmole). After stirring in the dark at room temperature for 18 h, TLC (developed using 50% acetone/chloroform) showed that most of the starting materials were consumed. The solvent was evaporated in vacuo. The solid was then triturated with ethyl ether to remove unreacted dinitrobenzoyl chloride; recrystallization from 5% $NaHCO_3$ solution afforded the final product in the dianion form, m.p. > 300°: ^{1}H NMR (400 MHz, DMSO-d_6) δ 11.06 (s, 1H), 9.25 (d, J = 1.6 Hz, 1H), 8.31 (s, 1H), 7.99 (dd, J = 8 Hz, J = 1.6 Hz, 1H), 7.03 (d, J = 8 Hz, 1 H), 6.59 (d, J = 9 Hz, 2H), 5.98 (dd, J = 9 Hz, J = 1.6 Hz, 2H), 5.88 (d, J = 1.6 Hz, 2H).

Alternative recrystallization of the impure solid product from ethanol afforded **4** in its neutral form (m.p. = 251–252°): ^{1}H NMR (400 MHz, DMSO-d_6) δ 11.26 (s, 1H), 9.21 (d, J = 2 Hz, 2H), 9.03 (t, J = 2 Hz, 1H), 8.50 (d, J = 1.6 Hz, 1H), 8.12 (dd, J = 8.4 Hz, J = 1.6 Hz, 1H), 7.33 (d, J = 8.4 Hz, 1H), 6.70 (d, J = 2.4 Hz, 2H), 6.63 (d, J = 8.8 Hz, 2H), 6.57 (dd, J = 8.8 Hz, J = 2.4 Hz, 2H); ^{13}C NMR (65.9 MHz, DMSO-d_6) δ 168.5, 162.2, 161.9, 159.7, 152.0, 148.2, 147.7, 140.0, 137.0, 129.2, 128.2, 127.7, 127.0, 124.7, 121.4, 115.3, 112.8, 109.6, 102.3; HRMS (CI, NH_3), m/e 542.0851 (MH^+, calc. 542.0836 for $C_{27}H_{16}N_3O_{10}$).

2.3. Instrumentation

Absorption and emission spectra were recorded using, respectively, a Beckman model DU-7 spectrophotometer and a model 48000 phase-shift fluorometer from SLM instruments, and employing published procedures [17]. Cyclic voltammograms were obtained using a model 273A potentiostat/galvanostat (EG&G APR) controlled by the EG&G M270A (version 4.0) software package (scan rate: 1 mV–5 V/s) [18]. The half-wave reduction potential determined for **3** (with solvent, DMF, dried over P_2O_5) was −0.89 V vs. SCE (reversible couple); this value is associated with the reduction of the dichlorotriazinyl moiety since the fluorescein moiety (**1** or **2**) is reduced at < −1.0 V vs. SCE. Irreversible oxidation of the fluorescein moiety was observed for **3** and **4**

in DMF, with $E_p \approx 0.95$ V, as well as irreversible reduction of **4** with $E_p = -0.74$ V (vs. SCE).

2.4. General

Stock solutions of 2.0 mM **3** and **4** were made in freshly distilled DMF solvent. For each measurement, a 10 μM dye solution was prepared by diluting a stock solution with buffer or other solvent. Buffer solutions consisted of 2.0 mM phosphate (K_2HPO_4/NaOH) (pH = 8.0) and 2.0 mM acetate/acetic acid (pH = 5.3). For the mixture of dye and PVP with varying R/D, aliquots of PVP stock solution were added to 10 ml of aqueous dye solution. For titration measurements, μl amounts of concentrated HCl and NaOH were used to adjust pH to the desired value. All spectrophotometric measurements were carried out at room-temperature on air-saturated samples.

2.5. Fluorescence methods

For fluorescence emission measurements, a 1 × 1 cm all-face-polished quartz cell was used for right-angle detection, and samples were excited at the blue edge of the visible absorption band of dye (~450 nm). The optical density at the excitation wavelength was ≤0.2 under all conditions. Fluorescence quantum yields (Φ_f) were determined by comparing the spectrally corrected emission intensity of the sample to that of a fluorescence standard using the following equation [19]:

$$\Phi_{f(s)} = \Phi_{f(r)} \frac{\int F_s(\lambda)d\lambda}{\int F_r(\lambda)d\lambda} \left(\frac{I_r}{I_s}\right)\left(\frac{n_s^2}{n_r^2}\right)$$

where $\int F_s(\lambda)d\lambda$ and $\int F_r(\lambda)d\lambda$ are the integrated emission intensities for the sample (s) and the reference (r), I_r/I_s is the ratio of light intensities absorbed by the two solutions at the excitation wavelength, and n_s and n_r are the refractive indices of the sample and the reference solutions, respectively. The fluorescence standard chosen for this study is the parent compound fluorescein, which has a known fluorescence quantum yield of 0.93 for aqueous solution (pH = 9) [20,21].

Fluorescence lifetimes were measured using the phase-modulation method [17,19,22]. The phase-shift and demodulation data were obtained for the intensity modulation frequency range of 2 to 190 MHz; data points at a given modulation frequency were generated from 6 measurements, each of which is a result of 100 repetitive signal acquisitions. A freshly prepared aqueous solution of glycogen, a light scatterer, was used as the lifetime reference. Emission decay data were tested for goodness of fit using multiple exponential functions as described [17]. Data were most successfully fit to biexponential decay functions; lifetimes associated with the largest components were reproduced with error limits of ±10%. The single-wavelength fluorescence polarization (anisotropy) data were obtained in the present work, using a dual-detector configuration (T-format detection) [19], where one detector is used for horizontally polarized emission (I) and the other for vertically polarized emission ($I_\perp$). Values of polarization and anisotropy were computed from the emission intensities using the relations and correcting for dispersion effects [22],

$$r = \frac{I_\parallel - I_\perp}{I_\parallel + 2I_\perp}$$

$$r = \frac{2P}{3-P}$$

For experiments with both **3** and **4** solutions (10 μM), the excitation wavelength was 450 nm; the emission was detected at 520 nm.

2.6. Molecular modeling

Molecular modeling was carried out using the software package QUANTA (Polygen software) with a CHARMm empirical energy calculation program on a Silicon Graphics Indigo 2 work station. The geometries of the dye molecules were optimized by the steepest decent and adopted-basis Newton–Raphson algorithms to minimize energy [23]. The dielectric constant of the medium was fixed at 78.5 (water). Energy minimization was carried out for 1000 steps or until an energy minimum was reached.

3. Results and discussion

3.1. Absorption and emission properties of fluorescein conjugates in water

Fluorescein derivative **3** (disodium salt) is a commercial material that has been used as a fluorescence labeling reagent for proteins, based on an assumed reaction of the triazine moiety with nucleophilic sites (e.g., lysine side chains) [24–27]. Compound **4** was obtained by condensation of **2** with 3,5-dinitrobenzoyl chloride and purified by isolation of the neutral form of the dye. The various states of protonation and tautomeric forms of the xanthenes are well known [28]. For fluorescein, pK_a values of 6.4, 4.3, and 2.1 have been determined for the sequence of protonations of the dianion to monoanion (Scheme 2), to neutral (zwitterionic and lactone tautomers), and to cationic forms, respectively [29].

Absorption and emission spectra for fluorescein and for the fluorescein conjugates in water are shown in Fig. 1. The absorption data, displayed further in Table 1 reveal modest differences among **1**, **3**, and **4**. The derivatives, substituted in the 9-position of the xanthene moiety, display a similar absorptivity associated with the long-axis-polarized transition in the visible, compared with the parent fluorescein

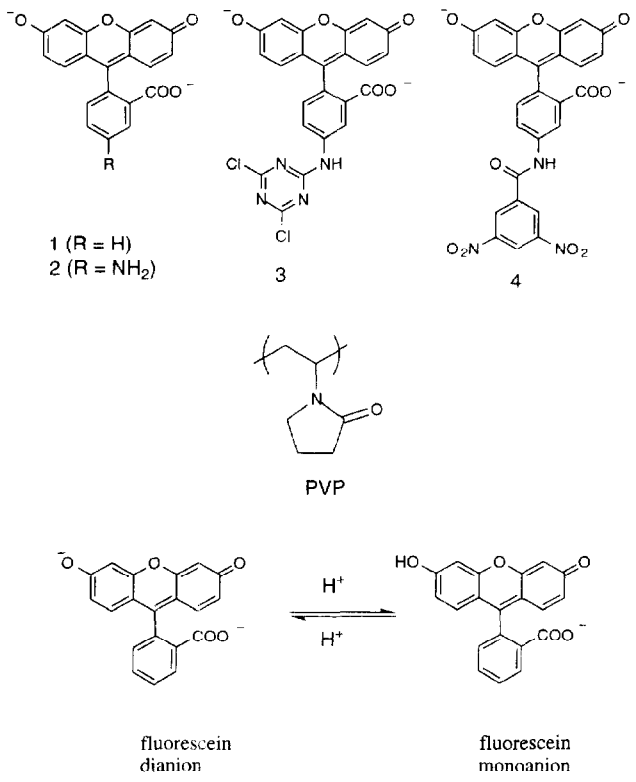

Scheme 2.

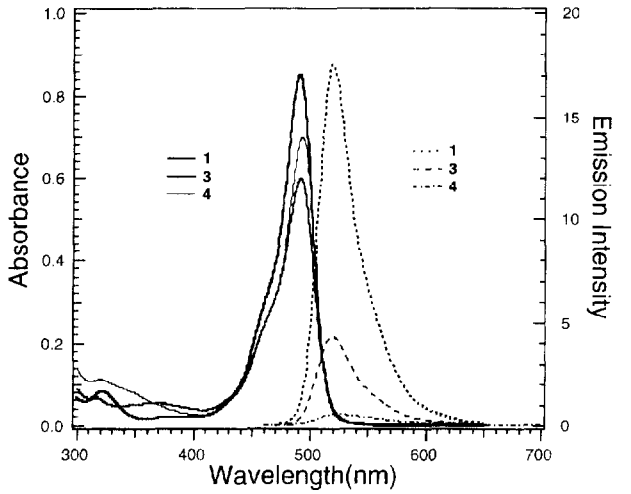

Fig. 1. Absorption and emission spectra for fluorescein and fluorescein conjugates, 10 μM in aqueous solution: 2.0 mM phosphate buffer (pH = 8.0); λ_{exc} = 450 nm.

(λ_{max} = 490 nm, ε = 76,900 M^{-1} cm^{-1}) and moderate enhancement of bands in the UV (350–380 nm). Consistent with earlier findings for **1** [29], alteration of the pH of aqueous solutions results in transformation of the dianion (λ_{max} = 491 nm) to the monoanion (with the development of two maxima at ca. 455 and 475 nm). Further acidification gives the neutral form of the conjugates, for which there is diminished absorption at 440–490 nm and, subsequently, a cationic species (λ_{max} = 440 nm) that is important below pH = 1.0. If the absorbance at a wavelength at which all forms

Table 1
Effect of pH on photophysical properties of fluorescein derivatives [a]

	pH	λ_a (nm)	ε (10^4 M^{-1} cm^{-1})	λ_f (nm)	Φ_f
3	11.0	491	7.4	520	0.26
	7.8	491	5.7	520	0.19
	5.9	455	2.8	520	0.13
		477	2.8		
	5.3	453	2.4	520	0.15
		475	2.3		
	2.0	439	2.9	523	0.082
	0.2	440	4.3	521	0.0095
4	11.0	492	8.6	522	0.012
	8.3	492	8.2	523	0.027
	7.1	491	6.1	524	0.092
	5.3	454	2.3	521	0.19
		477	2.3		
	4.0	449	1.3	521	0.11
	2.6	441	1.5	525	0.052

[a] 10 μM dye conjugate in aqueous solutions; for fluorescence measurements, δ_{exc} = 450 nm.

contribute is recorded as a function of pH (Fig. 2, inset), midpoints can be obtained for **3**, corresponding roughly to the known pK_a's of 6.4 and 4.3 for fluorescein [29]. The absorption data for the conjugates are thus quite similar to those obtained for **1**, indicating that the substituents that are positioned remotely are electronically coupled only weakly to the xanthene moiety (vide infra).

As shown in Fig. 1, the attachment of triazine and dinitrobenzamide groups to **1** results in fluorescence quenching. The higher level of quenching noted for **4** was investigated further through titration experiments. Shown in Fig. 3 are fluorescence curves generated for solutions at various intervals of pH. The conjugates showed nearly complete loss of emission

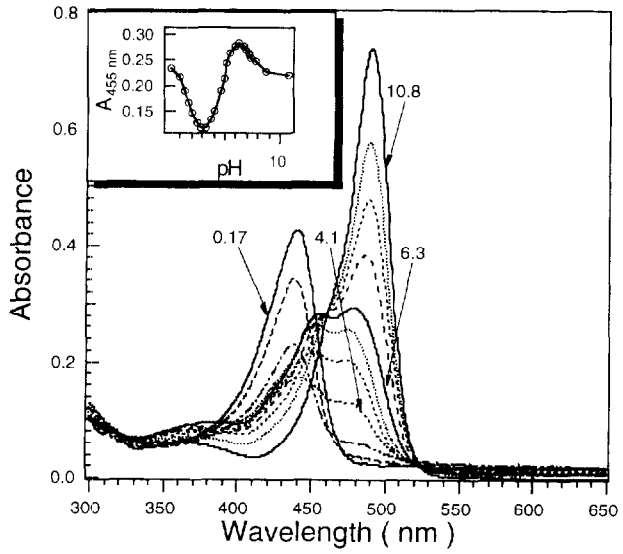

Fig. 2. Absorption spectra for 10 μM **3** in water as a function of pH. Inset: the change of absorbance at 455 nm where all protolytic forms absorb. The unlabeled curves correspond successively to pH values, 7.8, 7.3, 6.9, 5.6, 4.9, 2.6, and 1.7.

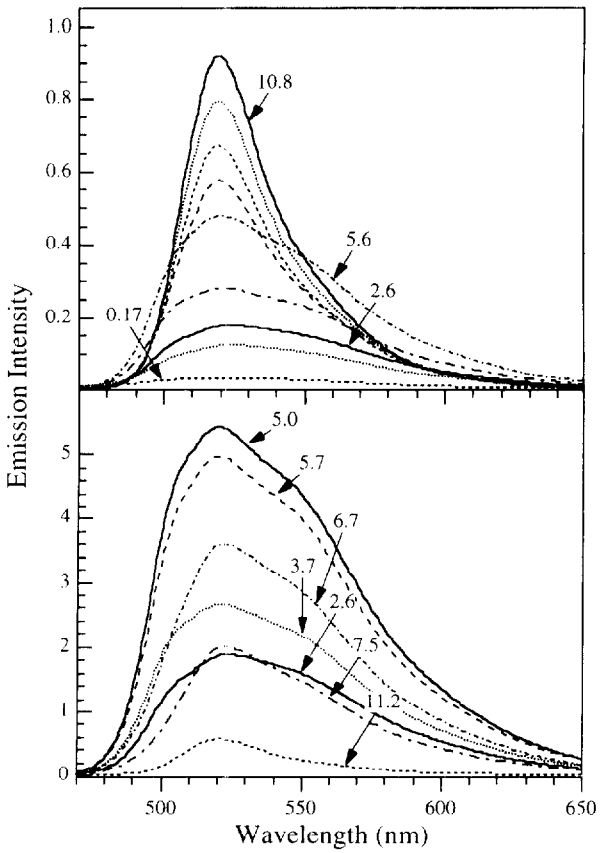

Fig. 3. Emission spectra for 10 μM **3** (upper panel) and **4** (lower panel) in aqueous solution at different pH (λ_{exc} = 450 nm).

at very acidic pH, consistent with the earlier findings that the fluorescence of neutral and cationic forms of fluorescein is inefficient [29]. The interesting pattern of fluorescence efficiency for **3** and **4** as a function of pH is also shown in the quantum yield and lifetime data shown in Table 2. Qualitatively, the pattern of emission yield and pH is consistent with the operation of two independent trends that have countervailing results. On the one hand, the dinitrobenzamide group is the more effective quencher of fluorescein emission over the pH range of 5–10, whereas the monoanion, the important species at lower pH (5.3), is less susceptible to quenching. These trends conspire to give the result that the lowering of pH for **3** leads to more significant emission quenching, while similar treatment for **4** results in fluorescence enhancement (Fig. 3). These trends will be discussed below in terms of the different influences on the driving forces involved for the mechanism of electron transfer quenching.

3.2. Absorption and emission properties of fluorescein conjugates in aqueous poly(vinyl-2-pyrrolidone) (PVP)

Aqueous solutions of the homopolymer of vinyl-2-pyrrolidone (PVP) have been found in many commercial products such as cosmetics, adhesives, pharmaceuticals, detergents and expanded plasma [30]. Some similarities to the transport protein, albumin, have been noted in the ability of moderate concentrations of PVP to solubilize or carry a variety of ligands including dyes, molecular iodine, hydrophobic anions, and some amino acids [13]. The polymer has particular affinity for anionic dyes, structures that incorporate the benzoic acid moiety, and phenols [31]. Several light scattering and viscosity studies have probed the process of PVP-ligand binding in detail. These investigations have shown that folding or crosslinking mechanisms that depend on the development of (non-covalent) ion-dipole and specific hydrogen bond interactions between PVP and ligands are important and responsible for a moderate contraction or shrinkage of the polymer coil in water [31–34].

Table 2
Effect of solvent, pH, and polymer binding by PVP on emission yields and lifetimes and kinetic parameters for fluorescein derivatives

	Solvent	Φ_f	τ_f (ns)	Decay rate constants (10^8 s^{-1})		
				k_f	k_{nd}	k_{et} [a]
3	ethanol [b]	0.71	4.2	1.7	0.69	0.69
	H_2O, pH = 5.3 [c]	0.15	2.9	0.52	2.9	–
	H_2O/PVP, pH = 5.3 [e]	0.19	3.8	0.50	2.1	
	H_2O, pH = 8.0 [d]	0.24	2.4	1.0	3.2	3.2
	H_2O/PVP, pH = 8.0 [e]	0.42	3.7	1.1	1.6	1.6
4	ethanol [b]	0.012	< 0.5	(1.7) [f]	> 140.0	> 140.0
	ethanol	0.25	2.4	1.1	3.1	–
	H_2O, pH = 5.3 [c]	0.19	2.2	0.88	3.7	–
	H_2O/PVP, pH = 5.3, [e]	0.20	2.5	0.81	3.2	–
	H_2O, pH = 8.0 [d]	0.046	< 0.5	(1.0) [f]	> 20.7	> 20.7
	H_2O/PVP, pH = 8.0, [e]	0.047	< 0.5	(1.0) [f]	> 20.7	> 20.7

[a] $k_{et} = k_{nd} - k_{nd}$ (**1**) (see text).
[b] With 0.05 N KOH.
[c] 2.0 mM acetate buffer solution.
[d] 2.0 mM phosphate buffer solution.
[e] R/D = 5000.
[f] Assumed value = k_f for **3** (dianion).

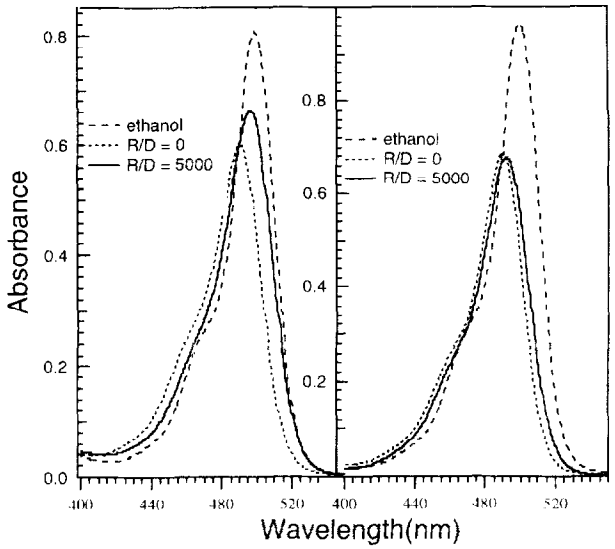

Fig. 4. Absorption of 10 μM **3** (left) and fluorescein (right) in different solvents; aqueous PVP solutions with 2.0 mM phosphate buffer (pH = 8.0, R/D concentration ratio specified); ethanol solution with 0.05 M KOH.

Table 3
Absorption and emission maxima for fluorescein derivatives in aqueous PVP at different pH and R/D [a]

	R/D [b]	λ_a (nm) ($\varepsilon \times 10^{-5}$ M^{-1} cm^{-1})		λ_f (nm)	
		pH = 5.3	pH = 8.0	pH = 5.3	pH = 8.0
3	0	454 (2.4)	490 (5.9)	520	520
		477 (2.4)			
	100	455 (2.1)	491 (6.1)	520	521
		477 (2.2)			
	1000	456 (2.0)	493 (6.2)	520	524
		477 (2.0)			
	3000	456 (2.0)	495 (6.2)	521	525
		478 (2.0)			
	5000	456 (1.9)	496 (6.2)	523	526
		478 (1.9)			
4	0	454 (2.8)	492 (7.6)	521	521
		477 (2.9)			
	100	456 (2.4)	492 (7.4)	522	523
		477 (2.5)			
	3000	455 (2.2)	494 (7.2)	522	525
		478 (2.2)			
	5000	456 (2.4)	495 (7.5)	521	526
		480 (2.6)			
	18000	459 (2.5)	499 (7.6)	524	527
		480 (2.8)			

[a] 10 μM dye conjugate; for fluorescence measurements, $\lambda_{exc} = 450$ nm.
[b] [PVP residue]/[dye] concentration ratio.

Absorption data for **3** and **4** in aqueous PVP are shown in Fig. 4 (including a comparison with **1**) and in Table 3. The data, presented in terms of [polymer residue]/[dye] concentration ratios (R/D), show that addition of PVP results in a perceptible red shift of the absorption maximum (e.g., 490 → 496 nm) for the dianions of **3** and **4**. The binding of dye conjugates is less apparent for the monoanions, which are important below pH = 6 and which result from xanthene

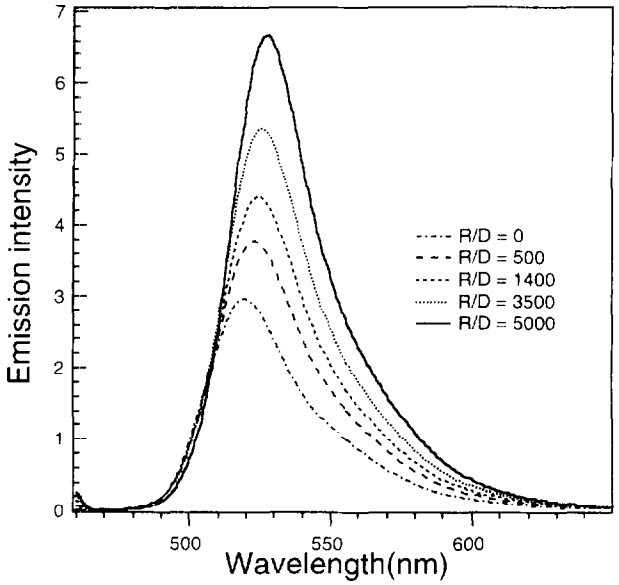

Fig. 5. Emission spectra for 10 μM **3** in aqueous solution with different R/D ratios; 2.0 mM phosphate buffer (pH = 8.0) ($\lambda_{exc} = 450$ nm).

ring protonation [28,29]. Fluorescence spectra are also perturbed on addition of PVP to aqueous solutions of **3** (Fig. 5). An enhancement in fluorescence yield of about 2-fold is observed for **3**, along with a 4 nm red shift of the emission maximum, for solutions having a large molar excess of polymer (R/D = 5000). A similar shift in the absorption maximum for **4** is observed on addition of PVP at pH = 8.0 (Table 3), although a PVP-induced enhancement of fluorescence intensity/yield is not observed for this conjugate (vide infra).

The equilibrium associated with the binding of conjugates by PVP was examined in a semi-quantitative way, using spectrophotometric techniques. The association can be represented in a simplified way as the binding of a polymer residue (R) and dye (D) (to form a complex),

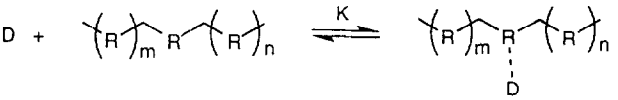

The binding isotherm that develops from emission data can be used to obtain a Benesi–Hildebrand double reciprocal plot [35,36] relating changes in emission intensity and polymer residue concentration. Using the Benesi–Hildebrand relation,

$$\frac{1}{\Delta\Phi} = \frac{1}{K} \cdot \frac{1}{[P]_0^m \Delta\Phi_\infty} + \frac{1}{\Delta\Phi_\infty}$$

where $\Delta\Phi$, $\Delta\Phi_\infty$ and $[P]_0^m$ represent a given change in fluorescence yield or intensity, the maximum change in emission yield and the total polymer residue concentration, respectively, the data (Fig. 6) can be used to obtain a binding constant, $K = 216$ M^{-1}.

For a polymer having a weight average molecular weight of 360,000 Da and a degree of polymerization of 3240, one can also compute from the value of K another constant for dye-polymer association, $K' = 0.07$ M^{-1}. Alternatively, if

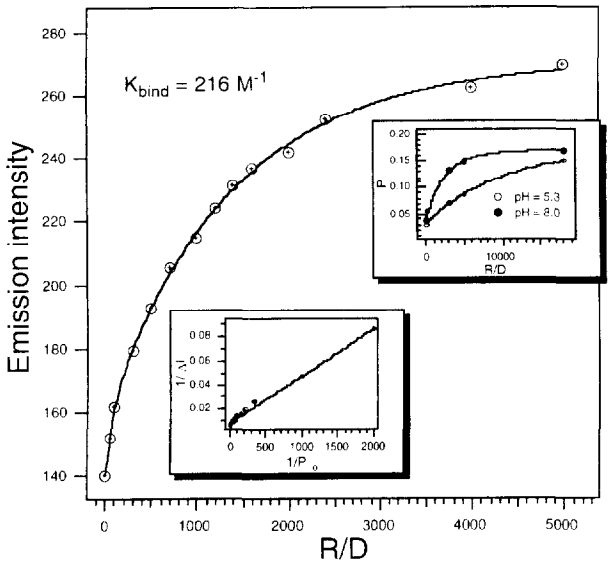

Fig. 6. Emission intensity of 10 μM **3** as a function of polymer residue to dye concentration ratios (R/D); 2.0 mM phosphate buffer (pH = 8.0) (λ_{exc} = 450 nm). Insets: Benesi–Hildebrand plot; fluorescence polarization of 10 μM **3** as a function of R/D.

one takes an estimate of the average number of residues which constitute a binding site (10) [32], an analogous equilibrium

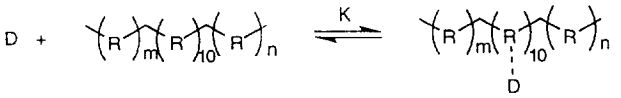

can be formulated and another approximate binding constant determined ($K'' = 21.6\ M^{-1}$). It should be pointed out, however, that multiple binding sites on the polymer chain are possible and that binding constant values do not have a precise stoichiometric significance. Previous examinations of dependences of binding on polymer molecular weight have shown that high affinity binding characteristics (polymer domain formation) for low molecular weight ligands are observed for PVP with average MW down to 5000 [32,33,37].

The polarization of fluorescence of **3** and **4** was examined also as a function of added PVP (Fig. 6). For **3**, values of the polarization, P, reached a plateau of 0.15–0.16 (corresponding to a peak value of the anisotropy, $r = 0.11$) for concentration ratios above 5000, indicative of virtually complete binding of emitting chromophores at that concentration of polymer. The rise in emission polarization is consistent with a substantial increase in the average hydrodynamic radius of the emitting species that results in polymer binding; i.e., the process of rotational diffusion that is largely responsible for depolarization is slowed for bound fluorophors which, in effect, become part of larger polymer segments [22].

3.3. Fluorescence quenching kinetics: singlet-state electron transfer for fluorescein conjugates

Fluorescence lifetimes and quantum yields were measured for **3** and **4** in water, as well as aqueous PVP solutions. The data are shown in Table 2. The phase-shift and demodulation data for emission were reasonably consistent with single exponential decays of fluorescence for the conjugates. However, somewhat more satisfactory fits to double-exponential decays were recorded, all having a second component amounting to a 5–10% contribution. This result may indicate that there is more than one conformation for the ligated structures that is distinctly photoactive or that slightly different binding sites (even with a distribution of lifetimes [38]) within PVP domains are important. For the present analysis, attention is paid primarily to the component from biexponential decay data representing the longer lifetime, which contributes $\geq 90\%$ to the total decay function. Unfortunately, the measurement of lifetimes was limited with current instrumentation to $\tau > 0.5$ ns, so that the data set for **4** could not be completed, requiring the setting of limits for decay times for basic conditions (Table 2).

In the general case in which electron-transfer competes with fluorescein fluorescence, along with other modes of non-radiative decay, a dissection of rate constants can be carried out using the following relations:

$$k_f = \frac{\Phi_f}{\tau_f}$$

$$k_{nd} = \frac{1 - \Phi_f}{\tau_f}$$

$$k_{nd} = k_{et} + k_{nr}$$

where Φ_f is the quantum yield of the fluorescence emission for the dye conjugates, τ_f is the lifetime for the emitting state, and k_f and k_{nd} are rate constants associated with fluorescence and non-radiative decay, respectively. The rate constant, k_{et}, represents that portion of the non-radiative decay that is ascribed to the proposed electron transfer mechanism; k_{nr} represents the rate of other non-radiative processes such as intersystem crossing [28].

The microscopic rate constants computed for **3** and **4** are listed in Table 3. For the dianion form of the parent fluorescein, the fluorescence quantum yield is close to unity in aqueous as well as alcohol solutions (with added base) ($\Phi_f = 0.93$ and 0.97, respectively [29]); i.e., the rate of nonradiative decay is small. As shown in the Tables, the fluorescence quantum yields for both **3** and **4** are generally below the value reported for the parent compound, and the lifetimes are shorter; compare for **1**, $\tau_f = 4.6$ and 4.1, respectively, for ethanol and for water solutions, pH = 8.0 [29] and the values for radiative and non-radiative processes that can be computed, $k_f = 2.3 \times 10^8\ s^{-1}$ and $k_{nd} = 1.7 \times 10^7\ s^{-1}$ for **1** in water (pH = 8–9). Given that the rate constant for non-radiative decay *not involving* electron transfer for the fluoresceins can be taken as $k_{nr} = k_{nd}$ for **1**, the non-radiative decay rate constants for the dianionic forms of **3** and **4** can be equated, to a very good approximation, with rates of intramolecular electron transfer; i.e., $k_{nd} \cong k_{et}$ (quenching is dominant and k_{nd} is large).

To evaluate the free energy change for the proposed electron transfer processes, the Weller equation [39,40] was employed along with data regarding the reduction (E_{red}) and oxidation (E_{ox}) half-wave potentials for the groups potentially involved:

$$\Delta G_{et} = 23.06(E_{ox} - E_{red}) - E_{00}$$

Based on an S_1–S_0 excitation energy (E_{00}) for fluorescein of 55.5 kcal/mol [41], free energy changes for electron transfer for **3** and **4** are relatively large and negative (−17.0 and −20.0 kcal/mol, respectively); i.e., electron transfer from the xanthene moiety to either of the electron acceptor groups is thermodynamically favorable. Electrochemical data show that the 3,5-dinitrobenzoyl moiety is the better electron acceptor, having a reduction potential of −0.76 V (vs. SCE) (reported for the model compound 3,5-dinitrobenzamide in DMF [42,43]) compared to −0.89 V vs. SCE for the dichlorotriazinyl moiety (see Section 2). The 0.13 V greater driving force for electron transfer for **4** thus accounts in part for the difference in the degree of fluorescence quenching for the conjugates (e.g., a lower quantum efficiency for fluorescence and faster non-radiative decay rate constants, k_{nd}, for **4**, pH = 8.0, Table 2). The suitability of an intramolecular electron transfer mechanism for excited state quenching has been similarly assessed for other systems having linkages of a chromophore (e.g., a porphyrin) and the dinitrobenzoyl moiety [44,45].

For both conjugates, the case for emission quenching via electron transfer is less unambiguously made for conditions in which the fluorescein monoanion is the fluorescent species. Thus, $\Phi_f = 0.15$ for **3**, and 0.19 for **4** in water (pH = 5.3), as compared to 0.37 for the fluorescein monoanion [29]. In as much as the non-radiative processes are inherently faster for the base chromophore **1** in its monoanion form, the competition from electron transfer quenching is not so obvious, and k_{et} is (at most) comparable in magnitude to k_{nr}. The less effective contribution of electron transfer to non-radiative decay for dye conjugates having the different charge type can also be attributed to a difference in driving force for electron transfer. The dianion form of both photoligands features the dissociation of the phenolic group which dramatically increases the electron density in the xanthene moiety (Scheme 2). Gouverneur et al. [46] studied the electrochemistry of a series of dyes in solution, among them fluorescein in both aqueous solution and aqueous/methanol (60/40, v/v) solution. They found that the oxidation half-wave potential is less positive for fluorescein in neutral water, where the dye is in the dianion form (0.78 V vs. SCE), on comparison with **1** in water/methanol (0.91 V vs. SCE), conditions which favor the monoanion. Although electron transfer for the monoanion of **3** is thermodynamically feasible according to the electrochemical data ($\Delta G_{et} = -14$ kcal/mol), the estimated driving force may be insufficient to result in a rate $> 10^8\ s^{-1}$ for the significant electron transfer distance required by the molecular linkage (vide infra).

The binding of the conjugates in aqueous PVP microdomains resulted in an increase in the fluorescence quantum yield and lifetime for **3**, but not for **4**. A decrease in the nonradiative decay constant (k_{nd}) of about 2-fold was computed for **3** (Table 2). This finding cannot be attributed to a previously documented medium dependence for xanthenes in less polar media [47,48] that leads to a slower rate of intersystem crossing, since k_{nd} remains a full order of magnitude larger for conjugate **3** in aqueous PVP, compared to **1** ($k_{nd} = 1.7 \times 10^7\ s^{-1}$). We attribute the effect of PVP binding to a decrease in the rate of electron transfer for conjugates bound in the polymer domain.

Further analysis of electron transfer rates included molecular modeling studies that provided energy-minimized structures for **3** and **4** (Scheme 3). These structures are relatively rigid, with center–center distances (xanthene ring to electron acceptor moiety) of 8.9 and 10.7 Å, respectively. The edge-to-edge through-bond distance of separation for donor–acceptor groups for both compounds was taken as 6.9 Å (xanthene 9-position carbon to pendant nitrogen), on the assumption that the acceptor moieties couple via their exocyclic nitrogen or amide functions which show π overlap with triazine or dinitrophenyl rings. Applying the Marcus relation [49,50],

$$k_{et} = 10^{13}\exp\{-\beta(r - r_0)\}\exp\{-\Delta G^{\neq}/RT\}$$

where

$$\Delta G^{\neq} = (\lambda + \Delta G^0)^2/4\lambda$$

3

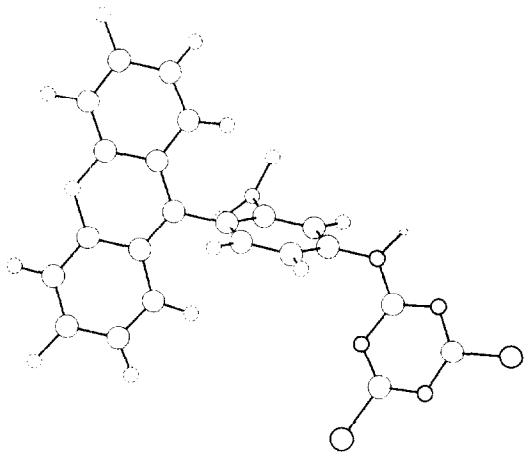

4

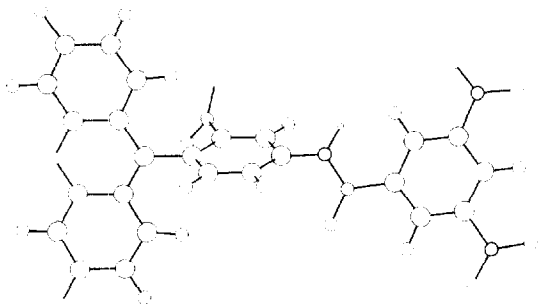

Scheme 3.

the rate constant for electron transfer can be expressed as a function of the free energy change for (ΔG^0), the reorganization energy (λ), and the distance of separation for donor and acceptor moieties ($r-r_0$). The reorganization term, λ, can in turn be factored into contributions associated with solvent reorientation during electron transfer (λ_{out}), and alterations in internal nuclear coordinates for the donor–acceptor structure (λ_{in}).

Using the rate constants for electron transfer, 3.2×10^8 and 1.6×10^8 s^{-1}, respectively, for **3** in aqueous solution and in aqueous PVP at pH = 8.0 (Table 2), incorporating a through-bond distance, $r-r_0=6.9$ Å and $\Delta G^0=0.74$ eV, and assuming a value for $\beta=1.0$ $Å^{-1}$ for the scaling parameter for distance dependence of electronic coupling [5,50], an estimate of the reorganization energy can be calculated—1.46 (33.7) and 1.57 (36.3) eV (kcal/mol) for **3** in water and in aqueous PVP, respectively. Given for **4** (also in water, pH = 8.0) a nominal value for a rate of non-radiative decay via electron transfer that is beyond the limits of determination from lifetime measurements, $k_{et}=5.0\times10^9$ s^{-1}, and, assuming in similar fashion, $\Delta G^0=-0.87$ eV, $\beta=1.0$ $Å^{-1}$, and $r-r_0=6.9$ Å, an estimate of the reorganization energy, $\lambda=1.16$ eV (26.8 kcal/mol) for the more reactive conjugate can be computed. Thus, with these assumptions, the more effective quenching of emission for **4** vs. **3** is finally attributed (along with the more favorable driving force, vide supra) to a smaller λ term and a closer approach to the ideal value, $\lambda=-\Delta G^0$, for which $\Delta G^{\neq}$ approaches zero (for **4** the value for the barrier to electron transfer is 0.018 eV). One rationale for this result is that a smaller λ_{out}, contributes to the reorganization energy for **4** and is associated with a larger effective radius for the charge that is delocalized in the electron transfer product (i.e., the dinitrobenzoyl group in **4** vs. the triazine group in **3**) [49,50].

The reduced rate of electron transfer for PVP-bound **3** can be understood in terms of an effect associated with the moderately higher reorganization energy that is computed from the rate data for electron transfer occurring the polymer microdomain. When donor–acceptor links are bound to polymer, nuclear motion associated with the ligand is restricted so that the freedom of an excited state to explore favorable nuclear configurations that are optimal for electron transfer is hindered (i.e., potentially leading to larger values of both λ_{out} and λ_{in}) [51]. Given the smaller reorganization energy term estimated for **4** (and a minimal value for $\Delta G^{\neq}$), a moderate alteration in λ associated with ligand-binding by polymer fails to result in a significant change in k_{et} or in a restoration of relative fluorescence intensity.

4. Conclusions

The fluorescein conjugates **3** and **4** show the characteristic absorption and emission properties of the parent compound **1**, although the emission quantum yields for both derivatives are lower than that of fluorescein under all conditions. For aqueous PVP solutions, both **3** and **4** are bound within the polymer microdomain and display typical red-shifts of absorption and emission maxima in the visible region and an increase in fluorescence polarization. Electron-transfer quenching of the fluorescence of **3** and **4** is proposed to compete with radiative decay, and other radiationless decay processes associated with the xanthene family of dyes. The higher level of electron transfer quenching for **4** (compared to **3**, k_{et} values, Table 2) is reflected in the reduction potentials for the two types of attached electron acceptor groups. Likewise, the higher electron–donor ability renders the xanthene dianion more subject to emission quenching than the monoanion form for both dye derivatives. The electron-transfer-mediated fluorescence for **3** is medium-dependent; upon binding to PVP in water (pH = 8.0), the rate of electron transfer decreases two-fold. The two fluorescein derivatives were studied in order to demonstrate a form of intramolecular interaction (emission quenching) that is counter to that observed for **2**, for which electron transfer quenching utilizes the fluorescein moiety as an electron acceptor [12]. This ensemble of fluorescein derivatives adds utility to the well established photoprobe behavior of the parent dye (**1**) in that fluorescence yield and lifetime, in general, report on the effects of microenvironment on a specific electron transfer process. Studies of electron transfer photoligands bound to organized assemblies or in the interior of globular proteins is a subject of continuing interest in our laboratory.

Acknowledgements

We thank the Division of Chemical Sciences, Office of Basic Energy Sciences of the U.S. Department of Energy for financial support of this work.

References

[1] G. Jones II, C.W. Farahat, C. Oh, J. Phys. Chem. 98 (1994) 6906.
[2] G. Jones II, Z. Feng, C. Oh, J. Phys. Chem. 99 (1995) 3883.
[3] G. Jones II, M. Farahat, D.X. Yan, in preparation.
[4] J. Deisenhofer, J. Norris (Eds.), The Photosynthetic Center, Academic Press, San Diego, CA, 1993.
[5] D.S. Bendall (Ed.), Protein Electron Transfer, BIOS Scientific Publishers, 1996.
[6] V.R. Vogel, E.T. Rubtsova, G.I. Likhtenshtein, K. Hideg, J. Photochem. Photobiol. A: Chem. 83 (1994) 229.
[7] G. McLendon, J. Feitelson, Meth. Enzymol. 232 (1994) 86.
[8] G. Tollin, J.K. Hurley, J.T. Hazzard, T.E. Meyer, Biophys. Chem. 48 (1993) 259.
[9] R.V. Stirling, Trends in Neurosci. (1986) 147.
[10] M. Prats, J. Teissié, J. Tocanne, Nature 322 (1986) 756.
[11] B. Gabriel, J. Teissié, J. Am. Chem. Soc. 113 (1991) 8818.
[12] C. Munkholm, D. Parkinson, D. Walt, J. Am. Chem. Soc. 112 (1990) 2608.
[13] P. Molyneux, in Water-Soluble Synthetic Polymers: Properties and Behavior, Vol. II, Chap. 2, CRC Press, Boca Raton, FL, 1984.
[14] G. Jones II, M.A. Farahat, S.R. Greenfield, D.J. Gosztola, M. Wasielewski, Chem. Phys. Lett. 229 (1994) 40.

[15] G. Jones II, D. Yan, S.R. Greenfield, D.J. Gosztola, M.R. Wasielewski, J. Phys. Chem. 101 (1997) 4939.
[16] G. Jones II, L.N. Lu, V.I. Vullev, D.J. Gosztola, S.R. Greenfield, M. Wasielewski, Bioorg. Med. Chem. Lett. 5 (1995) 2385.
[17] G. Jones II, C. Oh II, J. Phys. Chem. 98 (1994) 2367.
[18] G. Jones II, X. Qian, submitted.
[19] J.R. Lakowicz, Principles of Fluorescence Spectroscopy, Chaps. 3 and 5, Plenum, New York, 1985.
[20] G. Weber, F.W. Teale, J. Trans. Faraday Soc. 53 (1957) 646.
[21] P.G. Seybold, M. Gouterman, J. Callis, Photochem. Photobiol. 9 (1969) 229.
[22] J.R. Lakowicz, G. Laczko, H. Cherek, E. Gratton, M. Limkeman, Biophys. J. 46 (1984) 463.
[23] T. Clark, Handbook of Computational Chemistry, Wiley, New York, 1985.
[24] D. Blakeslee, M.G. Baines, J. Immunol. Meth. 13 (1976) 305.
[25] D. Blakeslee, M.G. Baines, J. Immunol. Meth. 17 (1977) 361.
[26] P.R. Banks, D.M. Paquette, Bioconjugate Chem. 6 (1995) 447.
[27] R. Siegler, L.A. Sternson, J.F. Stobaugh, J. Pharm. Biomed. Anal. 7 (1989) 45.
[28] D.C. Neckers, O.M. Valdes-Aguilera, in: D. Volman, G.S. Hammond, D.C. Neckers (Eds.), Advances in Photochemistry, Vol. 18, Wiley, New York, 1993.
[29] R. Sjoback, J. Nygren, M. Kubista, Spectrochim. Acta, Part A 51 (1995) L7.
[30] P. Molyneux, in: Water-soluble Synthetic Polymers: Properties and Behavior, Vol. 1, p. 146, CRC Press, Boca Raton, FL, 1983.
[31] P. Molyneux, S. Vekavakayanondha, J. Chem. Soc., Faraday Trans., 1, 82 (1986) 291 and 635.
[32] P. Molyneux, H. Frank, J. Am. Chem. Soc. 83 (1961) 3169.
[33] P. Molyneux, H. Frank, J. Am. Chem. Soc. 83 (1961) 3175.
[34] M. Nakagaki, S. Shimabayashi, Nippon Kagaku Kaishi, (1973) 207.
[35] R. Foster, in: Organic Charge-Transfer Complexes, Chap. 6, Academic Press, London, 1969.
[36] M. Barra, C. Bohne, J.C. Scaiano, J. Am. Chem. Soc. 112 (1990) 8075.
[37] Y.E. Kirsh, T.A. Soos, T.M. Karaputadze, Eur. Polym. J., 15 (1979) 223 and 639.
[38] J.R. Alcala, E. Ratton, F.G. Prendergast, Biophys. J. 51 (1987) 587.
[39] D. Rehm, A. Weller, Israel J. Chem. 8 (1970) 259.
[40] L. Eberson, in: Electron Transfer Reactions in Organic Chemistry, Springer Verlag, New York, 1987, pp. 27, 157.
[41] D.J. Lougnot, C.R. Goldschmidt, J. Photochem. 12 (1980) 215.
[42] V.M. Kazakova, V.I. Kovner, I.G. Makarov, V.B. Piskov, Zh. Strukt. Khim. 15 (1974) 1071.
[43] V.M. Kazakova, V.I. Kovner, I.G. Makarov, V.B. Piskov, Zh. Strukt. Khim. 17 (1976) 615.
[44] M. Sirish, B.G. Maiya, J. Photochem. Photobiol. A: Chem. 77 (1994) 189.
[45] K.D. Whitburn, M.Z. Hoffman, M.G. Simic, N.V. Brezniak, Inorg. Chem. 19 (1980) 3180.
[46] L. Gouverneur, G. Leroy, I. Zador, Electrochim. Acta 19 (1974) 215.
[47] G.R. Fleming, A.W.E. Knight, J.M. Morris, R.J.S. Morrison, G.W. Robinson, J. Am. Chem. Soc. 99 (1977) 4306.
[48] L.E. Cramer, K.G. Spears, J. Am. Chem. Soc. 100 (1978) 221.
[49] R.A. Marcus, Ann. Rev. Phys. Chem. 15 (1964) 155.
[50] G.J. Kavarnos, N.J. Turro, Chem. Rev. 86 (1986) 401.
[51] R.A. Marcus, J. Phys. Chem. 94 (1990) 4963.